

Influence of Chemical Compositions on the Properties of Random and Multiblock Sulfonated Poly(arylene ether sulfone)-Based Proton-Exchange Membranes

Cui Liang, Hitomi Hisatani, Tatsuo Maruyama, Yoshikage Ohmukai, Tomohiro Sotani, Hideto Matsuyama

Department of Chemical Science and Engineering, Kobe University, Kobe 657-8501, Japan

Received 7 May 2009; accepted 24 September 2009

DOI 10.1002/app.31489

Published online 1 December 2009 in Wiley InterScience (www.interscience.wiley.com).

ABSTRACT: The influence of chemical compositions on the properties of sulfonated poly(arylene ether sulfone)-based proton-exchange membranes was studied. First, we synthesized three different series of random SPAES copolymers using three kinds of hydrophobic monomers, including 4,4'-dihydroxydiphenylether, 2,6-dihydroxynaphthalene (DHN), and 4,4'-hexafluoroisopropylidenediphenol (6F-BPA) to investigate effects of hydrophobic components on the properties of SPAES membranes as proton-exchange membranes. Random SPAES copolymers with 6F-BPA showed the highest proton conductivity while random SPAES copolymers with DHN displayed the lowest methanol permeability among the three random copolymers. Subsequently, we synthesized multiblock SPAES using the DHN as a hydrophobic monomer and studied the effect of the length of hydrophilic segments in the multiblock SPAES copolymers on membrane performance. The

results indicated that longer hydrophilic segments in the copolymers led to higher water uptake, proton conductivity, and proton/methanol selectivity of membranes even at low humidity. In addition, the morphology studies (AFM and SAXS measurements) of membranes suggested that multiblock copolymers with long hydrophilic segments resulted in developed phase separation in membranes, and ionic clusters formed more easily, thus improving the membrane performance. Therefore, both the kinds of hydrophobic monomers and the length of hydrophilic segments in SPAES copolymers would influence the membranes performance as proton-exchange membranes. © 2009 Wiley Periodicals, Inc. *J Appl Polym Sci* 116: 267–279, 2010

Key words: proton-exchange membranes; sulfonated poly(arylene ether sulfone); random copolymer; multiblock copolymer

INTRODUCTION

Sulfonated poly(arylene ether sulfone) (SPAES) copolymers have been developed as an important candidate for a material of a proton-exchange membrane for polymer electrolyte membrane fuel cells, due to their high chemical and thermal stability, and excellent mechanical strength.¹ The sulfonated aromatic copolymers can be generally synthesized by post-sulfonation of commercial polymers or direct copolymerization of sulfonated monomers. Compared to post-sulfonation, the direct copolymerization of sulfonated monomers with other non-sulfonated aromatic monomers is more attractive,

because the degree of sulfonation can be precisely controlled by adjusting the ratio of sulfonated monomers to the non-sulfonated monomers in the polymerization.² Typically, sulfonated aromatic polymers are composed of two domain regions: hydrophilic and hydrophobic ones. The hydrophilic domains containing sulfonic acid groups provide membranes proton conductivity, while the hydrophobic domains composed of non-sulfonated monomers, supply the mechanical stability and restrict proton transport and water swelling.³ By using different monomers, diverse families of SPAES can be synthesized. Kim et al. synthesized SPAES copolymers derived from sulfonated 4,4'-dichlorodiphenyl sulfone (S-DCDPS), 4,4'-dichlorodiphenyl sulfone (DCDPS), and phenolphthalein (PP) and evaluated them as proton-exchange membranes for direct methanol fuel cells (DMFCs).⁴ Chikashige et al.⁵ synthesized a series of branched and cross-linked poly(arylene ether sulfone) ionomers containing sulfofluorenyl groups, and found that the branching and cross-linking were effective to improve the dimensional stability under wet conditions without losing their high thermal,

Correspondence to: H. Matsuyama (matuyama@kobe-u.ac.jp).

Contract grant sponsor: Special Coordination Funds for Promoting Science and Technology, Creation of Innovation Centers for Advanced Interdisciplinary Research Areas (Innovative Bioproduction Kobe), MEXT, Japan.

oxidative, and hydrolytic stability. Although there are already many studies on developing sulfonated aromatic copolymers as a material of a proton-exchange membrane, it is still a long way to apply these hydrocarbon-based aromatic copolymers to practical use. Better understanding on the relationships between the structures of hydrocarbon-based aromatic copolymers and properties of membranes are needed for designing the molecular structure of the copolymers. Most of the studies were usually focused on the comparison of copolymers with the same family, and the comparison was usually based on the effects of ion-exchange capacity (IEC). However, the investigation of relationship between a copolymer structure and a membrane performance should not only be conducted according to IEC, other factors, such as cross-linking,⁶ polymer backbone,⁷ should also be considered. Kim et al. investigated structure–property–performance relationships of directly copolymerized SPAES copolymers by introducing fluorine moieties or other polar functional groups into the copolymer backbone and observed that the fluorine incorporation increased the proton conductivity.⁸ Recently, Bae et al.³ studied the effect of sizes of hydrophobic components on the properties of SPAES membranes and found that small hydrophobic components induced high proton conductivities and high proton diffusion coefficients.

This study was carried out from two aspects to investigate the influence of chemical compositions on the properties of SPAES-based proton-exchange membranes. First, we synthesized three different series of random SPAES copolymers using three different kinds of hydrophobic monomers, 4,4'-dihydroxydiphenylether (DHDPE), 2,6-dihydroxynaphthalene (DHN), and 4,4'-hexafluoroisopropylidenediphenol(6F-BPA) to investigate the effect of hydrophobic components on the properties of SPAES membranes as a proton-exchange membrane. Second, we synthesized multiblock SPAES using the DHN as a hydrophobic monomer and studied the effect of the length of hydrophilic segments in the multiblock SPAES copolymers on membrane performance in comparison with the random SPAES copolymer. Water uptake, proton conductivity, methanol permeability, and morphology of various types of membranes were discussed.

EXPERIMENTAL

Materials

4,4'-Difluorodiphenyl sulfone (DFDPS), 6F-BPA were purchased from Aldrich. DHDPE was obtained from Tokyo Chemical Industry. DHN and potassium carbonate were obtained from Wako Pure Chemical Industries. Dehydrated dimethylsulfoxide (DMSO),

N-methyl-2-pyrrolidone (NMP), and toluene were also purchased from Wako Pure Chemical Industrials and used as received. The sulfonated 4,4'-difluorodiphenyl sulfone (SDFDPS) was synthesized in our laboratory using a process reported elsewhere.² Nafion 117 membrane was purchased from Aldrich.

Polymerization

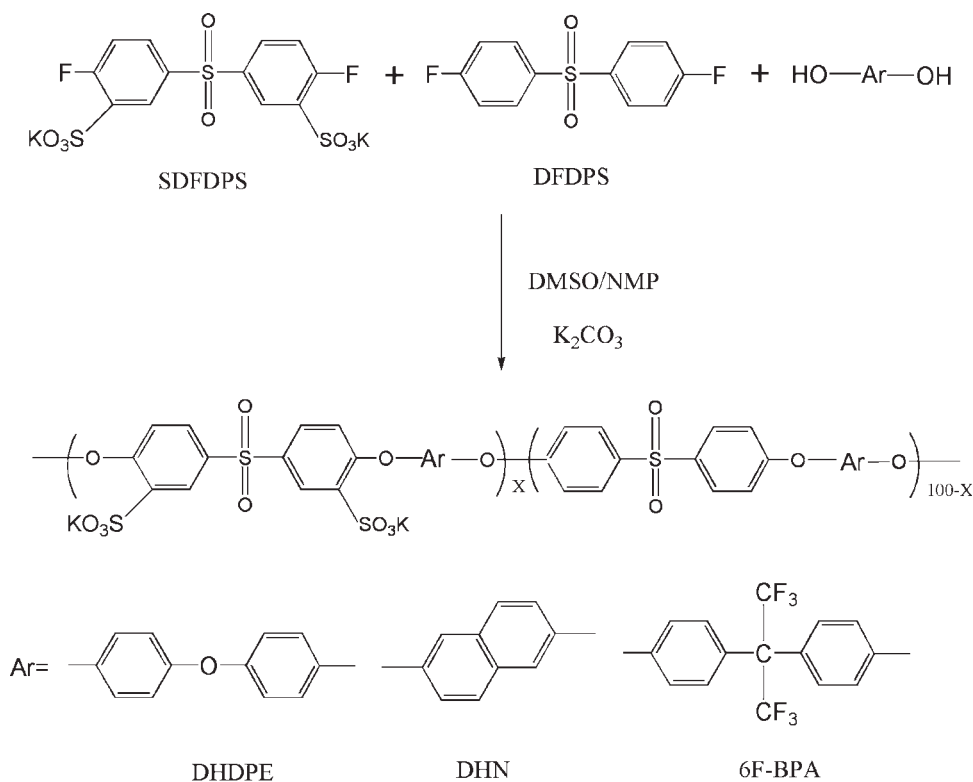
Syntheses of random SPAES copolymers (DHDPE series, DHN series, and 6F-BPA series) (Scheme 1)

Three series of random SPAES copolymers were synthesized via aromatic nucleophilic substitution (Scheme 1). The synthesis of random SPAES copolymers was conducted in a three-neck flask equipped with a nitrogen inlet and a Dean-Stark trap. A typical polymerization procedure of a DHDPE copolymer was as follows: SDFDPS (4.906 g, 10 mmol), DHDPE (4.044 g, 20 mmol), and DFDPS (2.542 g, 10 mmol) were dissolved in 60 mL dehydrated DMSO and NMP (1 : 1 in volume fraction). Toluene (10 mL) was used as an azeotropic agent. After the monomers were dissolved, potassium carbonate (4.146 g, 30 mmol) was added. The mixture was stirred at 150°C for 4 h to remove water from the reaction medium. After dehydration, the toluene–water mixture in the Dean-Stark trap was removed. The reaction temperature was raised to 165°C to remove the residual toluene in the flask. After the removal of the toluene, the polymerization was conducted for 24 h and a viscous polymer solution was obtained. After the reaction, the mixture was poured into a large quantity of deionized water to precipitate the synthesized random copolymer. The obtained polymer was then immersed in a 6 wt % HCl solution overnight to convert the copolymer into an acid form. The excess acid was washed by water and then the copolymer was dried in a vacuum oven at 80°C for 24 h. The DHN and 6F-BPA series copolymers were synthesized with DHN and 6F-BPA instead of DHDPE, respectively.

The syntheses of three series of random SPAES copolymers (DHDPE series, DHN series, and 6F-BPA series) were identified by ¹H-NMR as shown in Figure 1. Random copolymers in the same family with various IEC were prepared by controlling the ratios of the sulfonated monomer (SDFDPS) to the non-sulfonated monomer (DFDPS). The molecular weights and IEC of the prepared random copolymers are summarized in Table I.

Syntheses of multiblock SPAES copolymers (block-DHN series) (Scheme 2)

Multiblock SPAES copolymers were synthesized using the two-stage one-pot method (Scheme 2).⁹ The typical polymerization procedure was as



Scheme 1 Synthesis of random series copolymers.

follows: SDFDPS (3.679 g, 7.50 mmol) and DHN (1.586 g, 9.90 mmol) were dissolved in 40 mL dehydrated DMSO and NMP (1 : 1 in volume fraction) in a three-neck flask, which was equipped with a nitrogen inlet and a Dean-Stark trap. Toluene (10 mL) was used as an azeotropic agent. After the monomers were dissolved, potassium carbonate (3.11 g, 22.5 mmol) was added. The reaction medium was dehydrated at 25 kPa and 95°C for 5 h. After dehydration, the pressure was recovered to atmospheric pressure and the toluene–water mixture in the Dean-Stark trap was removed. Then, the pressure in the flask was reduced to 20 kPa and maintained for 1 h to remove the residual toluene in the flask. The pressure was then recovered to atmospheric pressure and the reaction was conducted at 140°C for 12 h. The resultant solution of hydrophilic oligomers was cooled to room temperature and used for the subsequent copolymerization. DHN (0.817 g, 5.10 mmol) and DFDPS (1.907 g, 7.50 mmol) were dissolved in 20 mL dehydrated DMSO and NMP (1 : 1 in volume fraction), and was added to the hydrophilic oligomer solution by syringe. Toluene (10 mL) was used as an azeotropic agent. The same method used for the syntheses of the hydrophilic oligomers was used to remove the water and toluene in the flask. Then the

polymerization proceeded at 160°C for 24 h. The reaction solution was poured into a large amount of deionized water to precipitate the synthesized multiblock SPAES copolymer. The obtained copolymer was then immersed in a 6 wt % HCl solution overnight to convert the copolymer into an acid form. The excess acid was washed by water and then the copolymer was dried in a vacuum oven at 80°C for 24 h.

The synthesized hydrophilic oligomer was confirmed by $^1\text{H-NMR}$ in $\text{DMSO-}d_6$, as shown in Figure 2. The hydrophilic oligomers with different sequence length were prepared by varying the initial monomer ratio of DHN/SDFDPSK to 1.32, 1.10, and 1.06, respectively. Three kinds of multiblock copolymers with different length of hydrophilic segments (block-DHN-1, block-DHN-2, and block-DHN-3) were synthesized. As the molar ratio of SDFDPS and DFDPS was fixed to 1, these three multiblock copolymers have similar IEC. Their molecular weights and IEC are summarized in Table II. The $^1\text{H-NMR}$ spectrum of a typical multiblock copolymer is also shown in Figure 2. All the chemical shifts of protons were assigned to the protons of the supposed chemical structure of the multiblock copolymers.

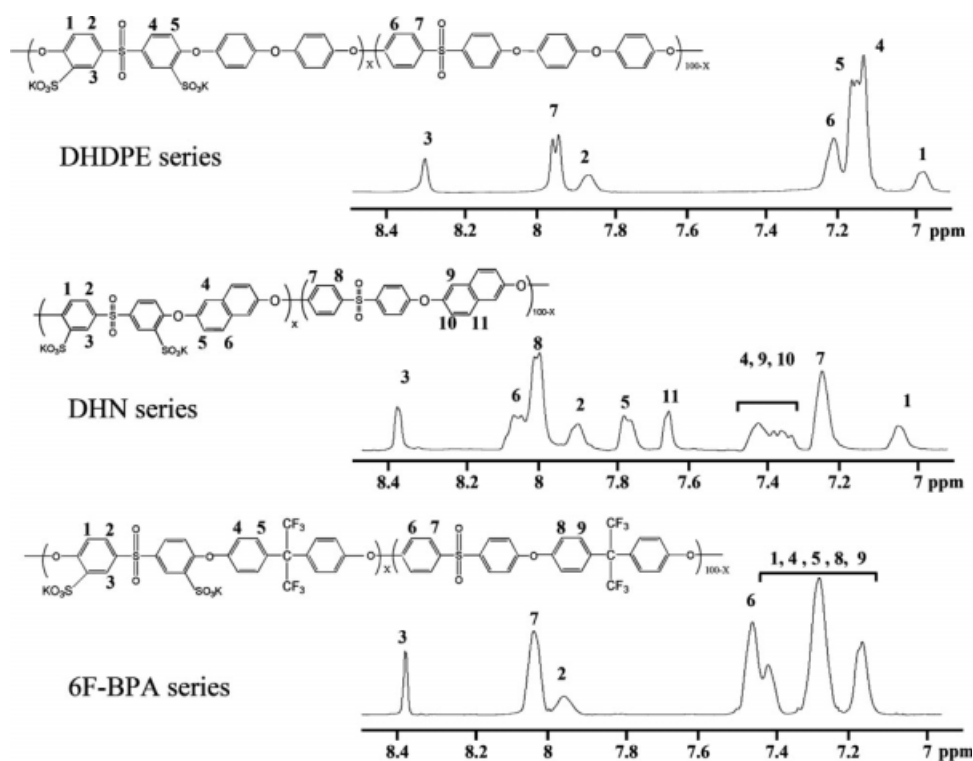


Figure 1 $^1\text{H-NMR}$ spectra of random polymers.

Membrane preparation

Membranes were prepared by casting 10 wt % polymer solutions in NMP on glass plates. They were dried at 80°C for 12 h, and at 100°C for another 48 h. The membranes were detached from the glass plates by immersing them into deionized water. The membranes were then stored in deionized water until use. The thickness of the wet membranes was about 100 μm .

Measurements

$^1\text{H-NMR}$ spectra were obtained on a Bruker AVANCE 500 NMR spectrometer. $\text{DMSO-}d_6$ was used as a solvent for the random copolymers and the hydrophilic oligomers. The multiblock copoly-

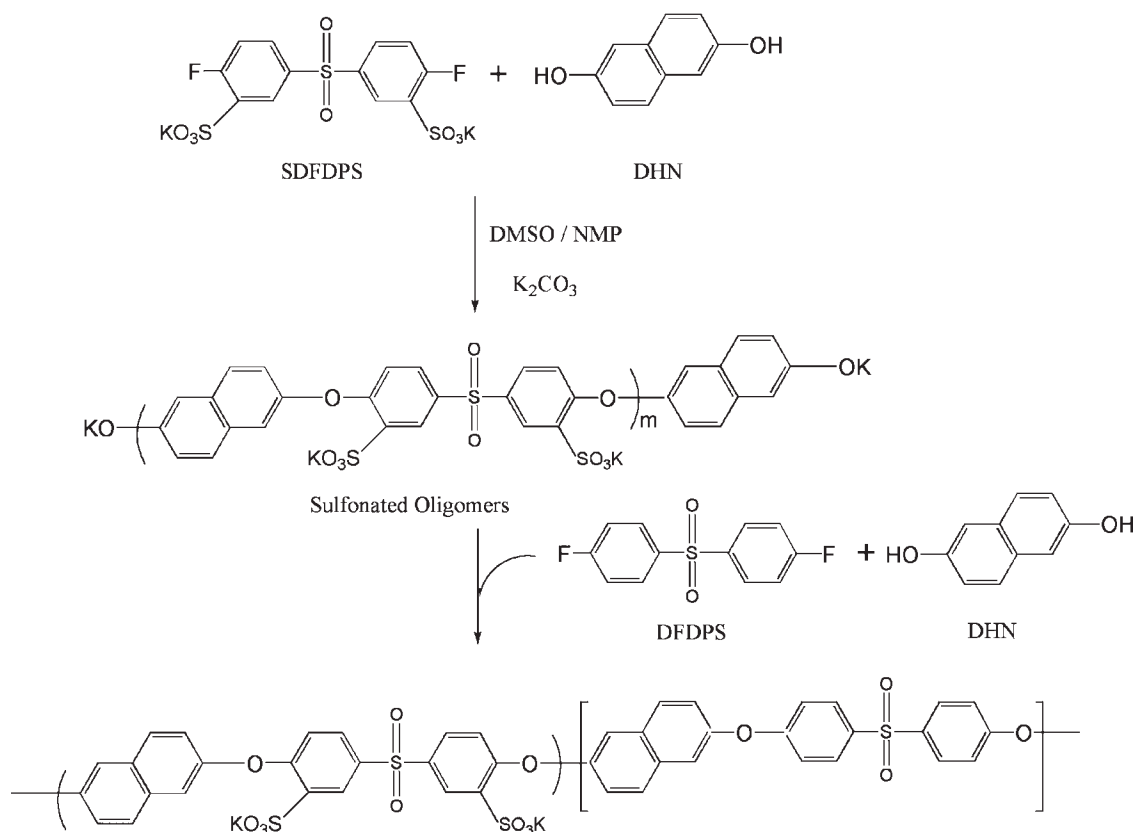
mers were measured in a 1 : 1 mixture of $\text{DMSO-}d_6$ and $\text{NMP-}d_9$.

The molecular weights of the copolymers and hydrophilic oligomers were measured using a gel permeation chromatography (GPC) system (LC-6A, Shimadzu, Japan) equipped with a UV detector (SPD-6AV, Shimadzu, Japan). NMP was used as a mobile phase at 40°C . A calibration curve was prepared by using molecular weight standards of polystyrene.

The IEC of the membranes was determined by a titration method.^{10,11} The water uptake was measured by a weight difference methodology. A wet membrane, which was soaked in deionized water for at least for 24 h, was weighed, dried in a vacuum oven at 100°C for 24 h, and then weighed again. The following equation was used for water uptake:

TABLE I
Molecular Weights and IEC of Random SPAES Copolymers

Copolymers	X (mol % SDFDPS)	M_w (kDa)	IEC (mmol/g)
DHDPE40	40	170	1.21
DHDPE50	50	92	1.52
DHDPE60	60	63	1.76
DHN40	40	410	1.20
DHN45	45	290	1.35
DHN50	50	271	1.49
DHN60	60	300	1.95
6F-BPA40	40	105	1.03
6F-BPA50	50	84	1.16
6F-BPA60	60	85	1.27



Scheme 2 Synthesis of multiblock series copolymers.

$$\text{Water uptake (\%)} = \frac{W_{\text{wet}} - W_{\text{dry}}}{W_{\text{dry}}} \times 100 \quad (1)$$

The proton conductivity of the membranes was measured by the AC impedance method. The proton

conductivity of the membranes at different temperature was measured by fixing the relative humidity of 100% and arranging the temperature from 25°C to 60°C. The proton conductivity of multiblock copolymers with different relative humidity was measured by fixing the temperature at 60°C and adjusting the

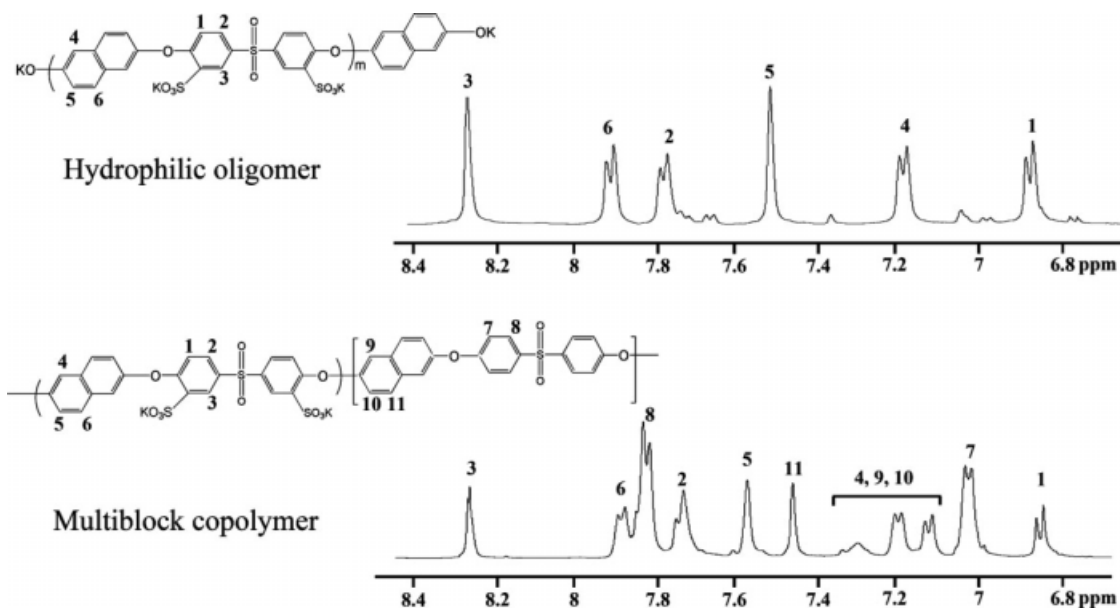


Figure 2 ¹H-NMR spectra of multiblock polymers.

TABLE II
Molecular Weights and IEC of Multiblock SPAES Copolymers

Polymer	Loaded moles of monomers for the synthesis [mmol]				Hydrophilic oligomers M_w (kDa)	Multiblock copolymers	
	First stage		Second stage			M_w (kDa)	IEC (mmol/g)
	SDFDPS	DHN	DFDPS	DHN			
Block-DHN-1	7.50	9.90	7.50	5.10	15	286	1.30
Block-DHN-2	7.50	8.25	7.50	6.75	25	144	1.32
Block-DHN-3	7.50	7.95	7.50	7.05	42	233	1.36

relative humidity from 30% to 100%. In both series of measurements, the samples were equilibrated in each temperature or relative humidity for 2 h and then the proton conductivity was measured. The conductivity (σ , S/cm) of the samples in the longitudinal direction was calculated by the following equation:

$$\sigma = \frac{l}{RS} \quad (2)$$

where l is the distance between the electrodes used to measure the potential ($l = 1$ cm), $R(\Omega)$ is the impedance of the membrane, and $S(\text{cm}^2)$ is the cross-sectional area of the membrane.

The methanol permeability was determined at room temperature (25°C) using a pair of glass chambers (each chamber was 20 mL in volume and had a cross-sectional area of 6.6 cm²), which contained water in one chamber and 1 mol/L MeOH solution in the other chamber. A membrane was set between the two chambers. The methanol permeability was obtained by periodically measuring the methanol concentration in the water chamber using a gas chromatograph (GC-8A, Shimadzu, Japan). The methanol permeability (P , cm²/s) through the membrane was given by,⁴

$$P = DK = \frac{1}{S} \frac{C_B(t)}{C_A(t - t_0)} V_B L \quad (3)$$

where $S(\text{cm}^2)$ and $L(\text{cm})$ are the membrane area and thickness, respectively, C_A (mmol/L) is the concentration of the methanol in the methanol chamber, $V_B(\text{mL})$ is the water volume in the water chamber, and t_0 is the time lag.⁴ D and K are the methanol diffusivity and partition coefficient between the membrane and the adjacent solution, respectively. DK is the permeability, which was evaluated from the slope of the linear line in a plot of the methanol concentration in the water chamber B (C_B , mmol/L) against the permeation time (t , s).

The surface morphology of the membranes was observed with an atomic force microscope (AFM, SPI3800N/SPA400, SII, Japan) in tapping mode. Thin membranes were prepared by spin-coating

1 wt % polymer solution onto a silicon wafer at 3000 rpm for 60 s at room temperature.

The small-angle X-ray scattering (SAXS) of dry membranes was measured using a Nano-Viewer RA-Micro 7 (Rigaku, Japan). The measurements were made with a Cu K α radiation generator ($\lambda = 0.1542$ nm) operating at 40 kV and 20 mA for 20 min at room temperature. The camera length used were 85.5 mm and 400 mm. Membranes were first stirred in 0.1 M CsCl solution for 24 h, then washed with deionized water and dried at 80°C overnight. The scattering vector q was defined by:

$$q = \frac{4\pi}{\lambda} \sin \theta \quad (4)$$

where λ and 2θ are the wavelength of the X-rays and the scattering angle, respectively.

The mechanical property of hydrated membranes was measured with a tensile apparatus (AGS-J, Shimadzu Japan) at room temperature. A hydrated membrane was cut into the size of 35 mm \times 5 mm and was set vertically between two pairs of tweezers with the distance of 20 mm. Then the membrane was extended at a constant elongation rate of 50 mm/min until it was broken.

RESULTS AND DISCUSSION

Membrane performances of random SPAES membranes

Three different series of random copolymers with various IEC were prepared using three different hydrophobic monomers by controlling the ratios of the sulfonated monomer (SDFDPS) to the non-sulfonated monomer (DFDPS). IEC and water uptake are closely related to the proton conductivity and methanol permeability of a proton-exchange membrane.¹² IEC indicates the density of ionizable hydrophilic groups in a membrane matrix, and the hydrophilic groups are responsible for the proton conductivity of a proton-exchange membrane.¹³ Water in a membrane serves as a carrier for the proton; however, high water uptake would weaken a membrane mechanically and lead to unacceptable dimensional

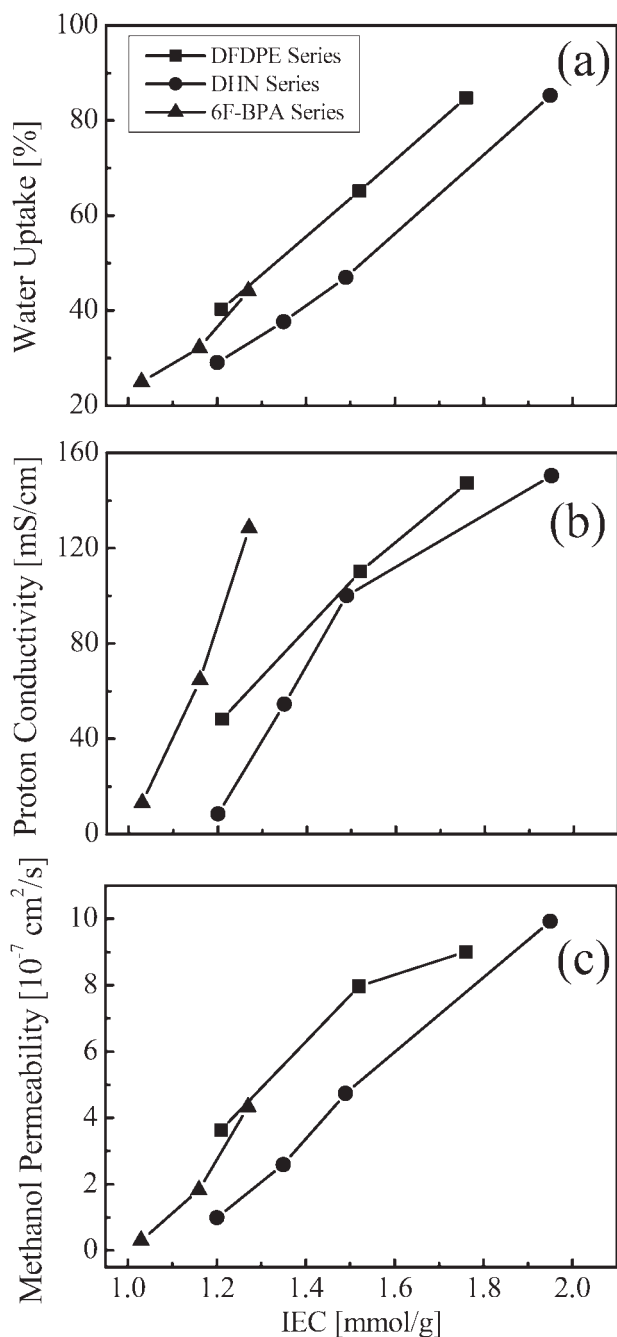


Figure 3 Effect of the ion-exchange capacity (a) on the water uptake, proton conductivity (b) and methanol permeability (c) of random series membranes. The proton conductivity was measured at 60°C, 100% relative humidity and the methanol permeability was at 25°C.

change.¹⁴ Adequate water uptake is, therefore, desired to exhibit sufficient proton conductivity. Figure 3(a–c) shows the water uptake, proton conductivity, and methanol permeability of the DHDPE series, DHN series, and 6F-BPA series SPAES membranes as a function of the IEC, respectively. The water uptake of the three series of the membranes increased with the increase of the IEC, because the sulfonic acid groups could keep water

in membranes. These results agree with the previous reports on the other kinds of copolymers.^{2,4} At a given IEC, the order of the water uptake of the membranes was DHDPE series > 6F-BPA series > DHN series.

The proton conductivity of three series membranes at 100% relative humidity and 60°C as a function of IEC is shown in Figure 3(b). The proton conductivity of the membranes increased with the increase of IEC. This increase of the proton conductivity can be explained by the increase of the sulfonic acid contents of the membranes and also the subsequent increase of the water content in the membrane. At given IEC, the order of the proton conductivity was 6F-BPA series > DHDPE series > DHN series. Even though the water uptake of DHDPE series was higher than 6F-BPA series, the proton conductivity of DHDPE series was lower than that of 6F-BPA series. This might be related to the phase separation of these copolymers, which provided a connected channel for the proton transport. Not only the amount of absorbed water but also the connection of hydrophilic domains would be important to the proton conductivity.³ The phase separation and the connection of hydrophilic domains will be discussed later. DHN series membranes with low water uptake showed lower proton conductivity than the other two series membranes.

The proton conductivity of DHDPE40, DHN40, and 6F-BPA50 membranes with similar IEC was studied as a function of the temperature. Figure 4 displays the Arrhenius plots of the conductivity of at temperatures ranging from 25°C to 60°C at 100% relative humidity. The data agreed with the Arrhenius law, indicating that the proton conductivity was dominated by a thermal activation process.¹⁵ The slope of the graphs can be used for the estimation of activation energy (E_a), the minimum energy required for the proton transport across the membrane, by fitting the Arrhenius equation, $\sigma = \sigma_0 \exp(-\frac{E_a}{RT})$ (where R is the gas constant and T is the absolute temperature).¹⁶ The activation energy of proton conductivity for DHDPE40, DHN40, and 6F-BPA50 was calculated to be 27.3 kJ/mol, 45.6 kJ/mol, and 30.2 kJ/mol, respectively. The activation energy of DHDPE40 membrane was a little lower than that of 6F-BPA50 membrane. This might be attributed to the flexible polymer backbone and higher water uptake of DHDPE40 membrane than that of 6F-BPA50. DHN40 membrane showed the highest activation energy, indicating that proton was difficult to be transported through membranes.

The methanol permeability of a proton-exchange membrane is another significant property for the application of a DMFC. High methanol permeation not only results in low fuel efficiency, but also causes low overall voltage performance. An ideal

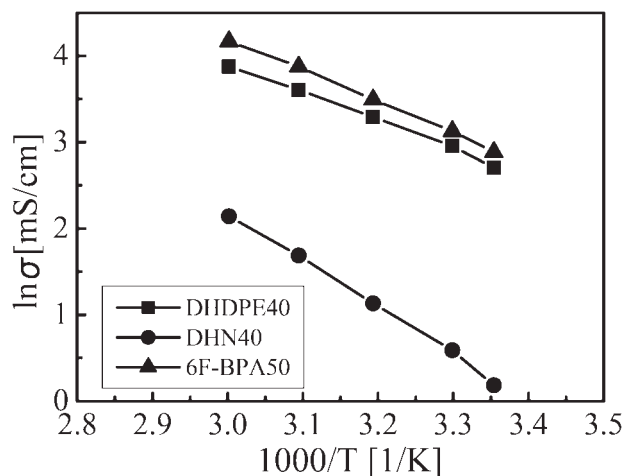


Figure 4 Effect of temperature on proton conductivity of DHDPE40, DHN40, and 6F-BPA50 membranes (at 100% relative humidity).

PEM for a DMFC is expected to have high proton conductivity and low methanol permeability.¹⁶ The methanol permeabilities of the three series membranes as a function of the IEC are shown in Figure 3(c). Similar to the water uptake, the methanol permeability increased with the increase of the IEC. The higher IEC of the copolymers meant higher water content and a higher amount of hydrophilic moiety in the membranes. The high water content and high amount of hydrophilic moiety mediated not only the proton transport but also the methanol transport through a membrane. In fact, the DHN40 membrane showed the lowest methanol permeability because of the lowest water uptake among DHDPE40, DHN40, and 6F-BPA50 membranes that had similar IEC.

Proton/methanol selectivity is defined as the ratio of the proton conductivity to the methanol permeability. Generally, the higher the selectivity is, the better the membrane performance is.¹⁷ Figure 5 shows the proton conductivity of DHDPE series, DHN series, and 6F-BPA series membranes (at 25°C, 100% relative humidity) as a function of the methanol permeability (at 25°C). The slopes of the solid lines correspond to the selectivities of the membranes. Obviously, 6F-BPA series membranes had highest selectivity among the three series membranes. There was little difference between the selectivities of DHDPE series and DHN series membranes. This might indicate that in these membranes the mechanism of the proton transport is the same with that of methanol transport.

Morphology of random SPAES membranes

In sulfonated aromatic copolymers for a proton-exchange membrane, there are generally two domains: hydrophilic domains containing sulfonic

acid groups, and hydrophobic domains composed of non-sulfonated monomers. The geometric distribution of hydrophilic and hydrophobic domains in a membrane has been considered to influence the membrane property.¹⁸ The sulfonic acid groups in a membrane may assemble into ionic clusters as a result of the phase separation of a copolymer and form ionic channels in a membrane, both of which benefit the proton transport through a membrane.¹⁹ Thus, the morphology study of proton-exchange membranes is of great importance. To evaluate the phase separated structures in the present SPAES copolymers, we carried out AFM and SAXS measurements.

To investigate the effect of hydrophobic components on the morphology of random SPAES membranes, the surface morphology of random copolymers (DHDPE40, DHN40, 6F-BPA50), and Nafion was observed by AFM in tapping mode at 30% relative humidity (Fig. 6). Random copolymers inspected (DHDPE40, DHN40, and 6F-BPA50) had similar IEC (approx. 1.2 mmol/g). The dark regions in the phase images, which were assigned to softer regions, represent the hydrophilic parts of the membrane, while the bright regions were assigned to the hydrophobic parts.^{20,21} These phase images suggested that for 6F-BPA membrane, the hydrophilic domains and hydrophobic domains were larger than those of DHDPE40 and DHN40 membranes, indicating the developed phase separation in 6F-BPA membrane. When fluorine moieties were incorporated into the copolymer backbone, it could increase the hydrophobicity of the backbone and promote the phase separation.⁸

While the AFM measurements provided information about the surfaces of the membranes, SAXS measurements were useful in investigating the bulk

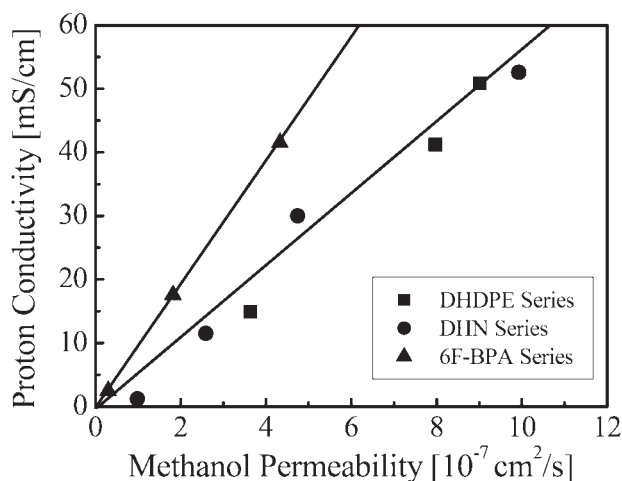


Figure 5 Proton conductivity (at 25°C, 100% relative humidity) of random series membranes as a function of methanol permeability (at 25°C).

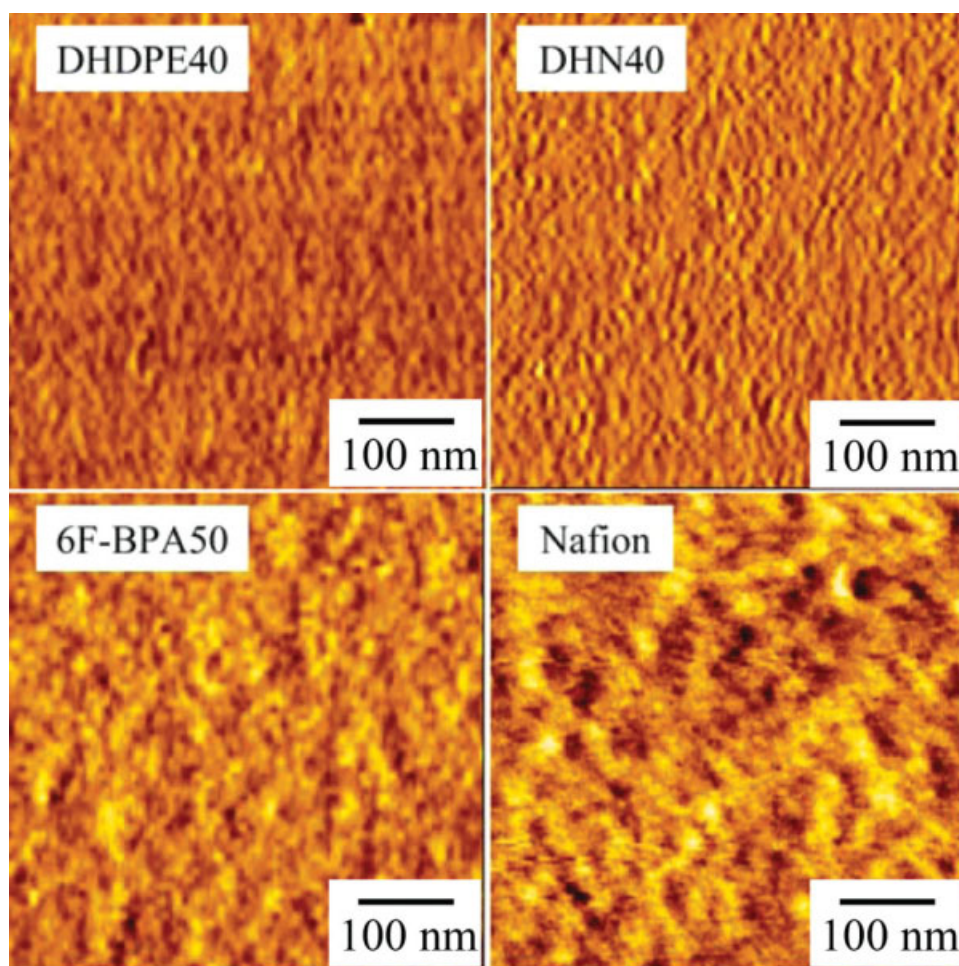


Figure 6 AFM phase images of spin-coated polymers of DHDPE40, DHN40, 6F-BPA50, and Nafion at room temperature with relative humidity of 30%. [Color figure can be viewed in the online issue, which is available at www.interscience.wiley.com.]

morphology of the membranes.²² The SAXS profiles of the dry DHDPE40, DHN40, 6F-BPA50, and Nafion 117 membranes are shown in Figure 7. An ionomer peak was observed at a q -value of approx. 1.9 nm^{-1} for the Nafion 117 membrane, while shoulder-like profiles were obtained for DHDPE40, DHN40, and 6F-BPA50 membranes. The shoulder-like profile was more pronounced for 6F-BPA50 membrane when compared with other membranes. These results implied the presence of the nano-scale periodic structure, like a phase separated structure, in 6F-BPA50 membrane, which is consistent with the AFM result.

Comparison of multiblock SPAES with random SPAES membranes

To date, many reports suggested that the phase separation of copolymers is significant for the proton conductivity of a proton-exchange membrane. Our present investigation described earlier also indicates the significance of the phase separation in the

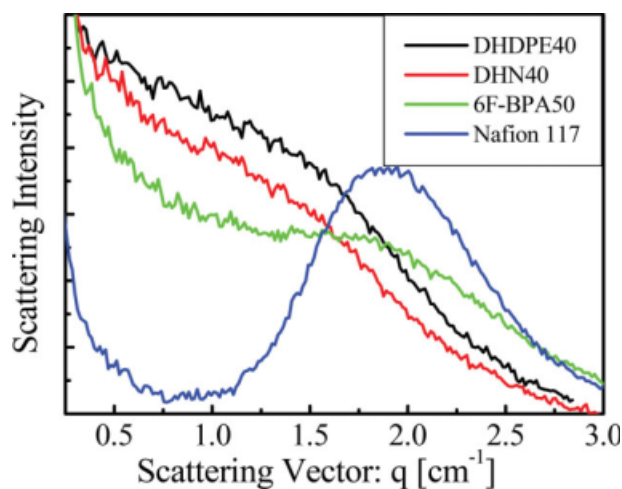


Figure 7 SAXS profiles of random DHDPE40, DHN40, 6F-BPA50, and Nafion 117 at 25°C. [Color figure can be viewed in the online issue, which is available at www.interscience.wiley.com.]

TABLE III
Characterization of Random DHN45, Block-DHN-1, Block-DHN-2, and Block-DHN-3 Membranes

Copolymer	Random DHN45	Block-DHN-1	Block-DHN-2	Block-DHN-3
IEC (mmol/g)	1.35	1.30	1.32	1.36
Water uptake (%)	37.6	52.8	55.8	79.6
Tensile strength (MPa)	26.6	17.1	14.6	11.3
Proton conductivity ^a (mS/cm)(60°C)	55	136	156	222
Activation energy (kJ/mol)	36.8	27.1	19.7	15.9
Methanol permeability (10 ⁻⁷ cm ² /s)	2.59	6.79	7.23	8.91

^a Relative humidity was 100%.

SPAES copolymer. However, the sulfonic acid groups in the random SPAES disperse over the backbone of the copolymers randomly and the random dispersion of the sulfonic acid groups was not thought to be effective for the phase separation in the SPAES copolymer. Thus, a multiblock copolymer has been attracted as a material alternative to a random copolymer for a proton-exchange membrane. Multiblock copolymers, which are usually composed of hydrophilic repeated segments and hydrophobic repeated segments, are likely to develop phase separation and to form ionic channels by connecting compartment-like structures in a membrane. By controlling the sequence length of the hydrophilic segments, phase separated structures with different sizes could be obtained. In the second part of this study, we adopted DHN series copolymer and synthesized three multiblock SPAES with similar IEC and with different length of hydrophilic segments. As DHN series random SPAES membranes showed the lowest methanol permeability among the present three series of random SPAES membranes, DHN was used as a hydrophobic monomer in the multiblock copolymerization. The effect of the length of hydrophilic segments in the multiblock copolymers on the performance of SPAES membranes was discussed and compared to the random DHN copolymer.

Water uptake, proton conductivity, and methanol permeability of multiblock SPAES membranes

Three multiblock copolymers (block-DHN-1, block-DHN-2, and block-DHN-3) synthesized with different molecular weights of hydrophilic oligomers were compared. For comparison, random DHN copolymer (DHN45) was also synthesized. These four copolymers had similar IEC (approx. 1.3 mmol/g). The water uptake, tensile strength, proton conductivity, activation energy, and methanol permeability of the multiblock and random SPAES membranes are summarized in Table III. Interestingly, the water uptake of the multiblock SPAES membranes increased with the increase of the hydrophilic segment length in the

copolymers. The water uptake seems to greatly depend on the morphology of the membranes, because they had similar IEC. The tensile strength of these membranes progressively deteriorated with the increase of the water uptake of the membranes. Higher water uptake of the membrane resulted in more flexible polymer chain and led to lower tensile strength.

The influence of temperature on the proton conductivity of the random DHN45, and multiblock block-DHN-1, block-DHN-2, block-DHN-3 was investigated, as shown in Figure 8. Plots are fitted linearly for E_a determination. The activation energy of the proton transport for DHN45, block-DHN-1, block-DHN-2, and block-DHN-3 was calculated to be 36.8 kJ/mol, 27.1 kJ/mol, 19.7 kJ/mol, and 15.9 kJ/mol, respectively. Even though monomers used and IEC of the copolymers were almost the same, the length of the hydrophilic segment of the copolymers induced large differences in the activation energy of the proton transport.

Random copolymers usually show satisfactory performance under high relative humidity, but they lose the performance drastically at low relative

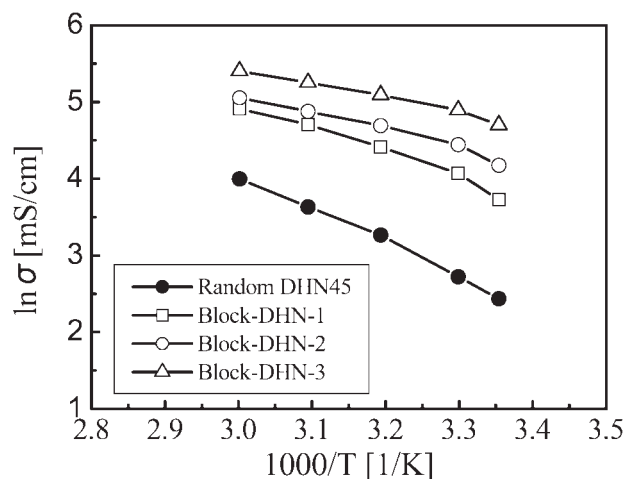


Figure 8 Effect of temperature on proton conductivity of random DHN45, multiblock series membranes (at 100% relative humidity).

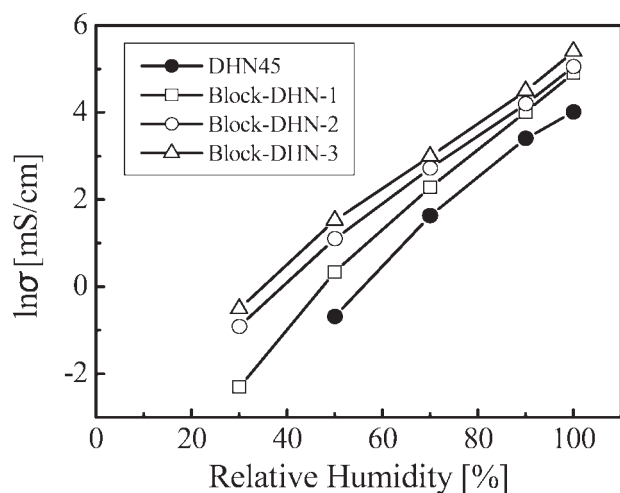


Figure 9 Effect of relative humidity on proton conductivity of random DHN45 and multiblock series membranes (at 60°C).

humidity.²³ The proton conductivity as a function of relative humidity for the random DHN45, and multiblock block-DHN-1, block-DHN-2, and block-DHN-3 was investigated (Fig. 9). The proton conductivity of the random DHN45 dropped significantly with the decrease of relative humidity. At the relative humidity of 30%, the proton conductivity was too low to be measured. Under low relative humidity, the scattered hydrophilic domains in the membranes would lack the connectivity of the hydrophilic domains and result in low proton conductivity.²⁴ Although the proton conductivity of the multiblock copolymers dropped with the decrease of the relative humidity, the multiblock copolymer especially with the longer length of the hydrophilic segment showed relatively high proton conductivity at low relative humidity.

All of the proton conductivity of membranes in this study was measured in the in-plane direction of the membranes; further study is needed to measure the proton conductivity in the transverse direction of the membranes.

The methanol permeability of the random DHN45 and multiblock DHN membranes is also listed in Table III. The increase of the hydrophilic segment length in the copolymer increased the methanol permeability of the membranes. This would be related to the increased water content and the connection of ionic clusters formed in the multiblock DHN membranes. The high water content and connection of ionic clusters allow not only the proton transport, but also the methanol transport through a membrane. The proton conductivity (at 25°C, 100% relative humidity) of the membranes was plotted as a function of the methanol permeability (at 25°C) in Figure 10. Despite the increase of the methanol permeability, the increase of the

hydrophilic segment length in the multiblock copolymer improved not only the proton conductivity but also the proton/methanol selectivity of the membrane.

Morphology of multiblock SPAES membranes

As discussed earlier, the morphology of the random SPAES copolymers and the AFM phase observations of random DHN45, block-DHN-1, block-DHN-2, and block-DHN-3 copolymers were conducted (Fig. 11). These four copolymers had similar IEC (approx. 1.3 mmol/g) and the block copolymers had different length of the hydrophilic segments. Compared to the random DHN45 copolymer, all the multiblock copolymers showed more marked phase separation. However, the increase of the hydrophilic segment length in the copolymers did not induce any distinct difference in the surface morphology of the copolymers.

SAXS profiles of block-DHN-1, block-DHN-2, and block-DHN-3 membranes are shown in Figure 12. The ionomer peak shifted to slightly higher q -value and the ionomer peaks became much clear with the increase of the hydrophilic segment length in copolymers. The peaks in the SAXS profiles indicated that the length of hydrophilic segments promoted the formation of nano-scale periodic structures presumably with phase separation. Assuming that the periodic structure in the copolymers was the spherical cluster of the hydrophilic parts, the Bragg distance, which referred to the center-to-center distance between two ionic clusters, decreased with increasing the hydrophilic segment length. Yang and Manthiram²² reported that the increase in the number of ionic clusters resulted in a small Bragg distance and high proton conductivity of SPEEK. In

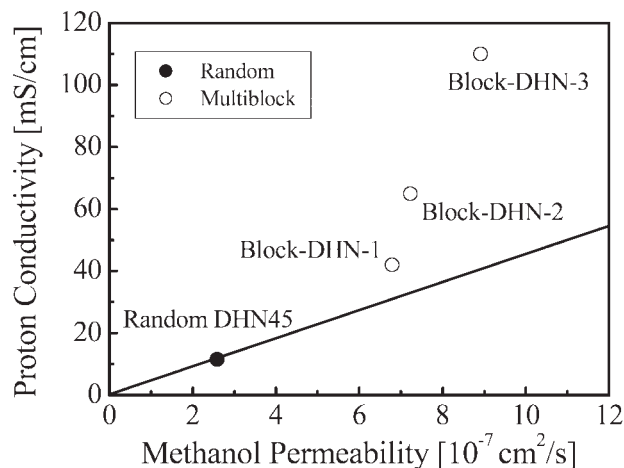


Figure 10 Proton conductivity (at 25°C, 100% relative humidity) of random DHN45 and multiblock series membranes as a function of methanol permeability (at 25°C).

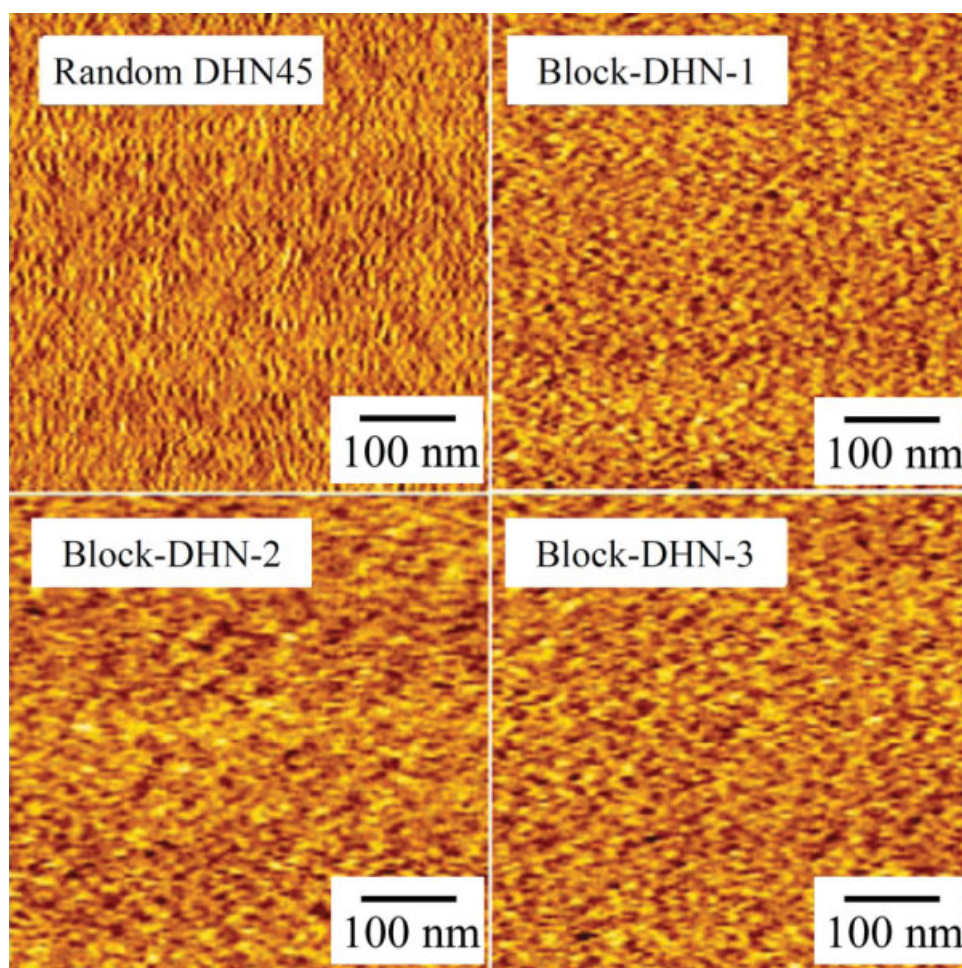


Figure 11 AFM phase images of spin-coated polymers of random DHN45, block-DHN-1, block-DHN-2, and block-DHN-3 at room temperature with relative humidity of 30%. [Color figure can be viewed in the online issue, which is available at www.interscience.wiley.com.]

this study, there was also a potential that long length of the hydrophilic segments increased the number of ionic clusters. That might be why we also observed the shortened Bragg distance in the multiblock copolymer with long hydrophilic segments and obtained the high proton conductivity of the membrane.

The AFM and SAXS results suggested that the multiblock structure of copolymers developed the phase separation and formed ionic clusters more easily in the membranes than the random copolymers. This phase separated structure might account for the improved performance in the water uptake and proton conductivity of the multiblock copolymers.²³ In addition, the long hydrophilic segment in the copolymers had potential to serve as a connector between ionic clusters in the copolymers, not only as an ionic cluster. Indeed, it was proposed that a continuous water network and mobile freezable water were essential for the proton transport through a membrane, because they provide a pathway for the protons or vehicles to transport the protons.²⁵ The

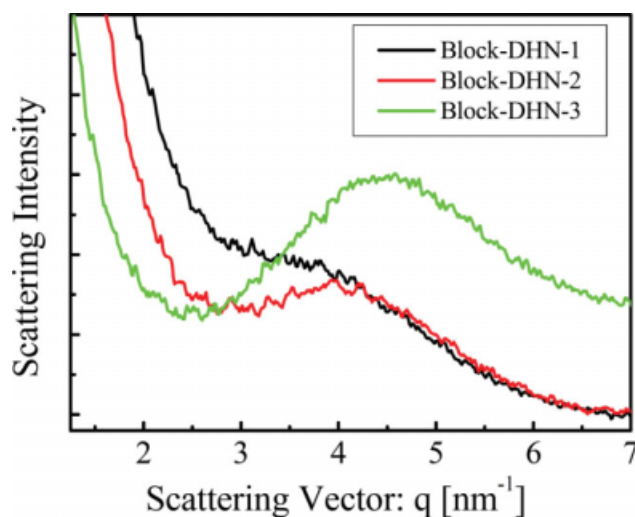


Figure 12 SAXS profiles of multiblock block-DHN-1, block-DHN-2, and block-DHN-3 at 25°C. [Color figure can be viewed in the online issue, which is available at www.interscience.wiley.com.]

shorter distance between ionic clusters, which was observed by the SAXS analyses, also helped the proton transport between the ionic clusters. This investigation on the length of the hydrophilic segments in SPAES copolymers suggested that with an increase in hydrophilic segment length, the degree of phase separation and the connectivity between the hydrophilic domains would increase.²⁶ As a result, the proton conductivity of the multiblock copolymer increased even at low humidity.

CONCLUSION

Three series of random sulfonated poly(arylene ether sulfone) were synthesized to study the effect of hydrophobic components of copolymers on the properties of proton-exchange membranes. The SPAES copolymers synthesized using 4,4'-hexafluoroisopropylidene -diphenol (6F-BPA series) as a hydrophobic monomer showed higher proton conductivity than SPAES copolymers using 4,4'-dihydroxydiphenylether (DHDPE series) and 2,6-dihydroxynaphthalene (DHN series). Using DHN as a hydrophobic monomer, three multiblock copolymers with different hydrophilic segment length were synthesized to investigate the influence of the hydrophilic sequence length on the properties of the multiblock SPAES membranes. Long length of the hydrophilic segment in the multiblock copolymers resulted in high proton conductivity and high proton/methanol selectivity even at low humidity, presumably due to the developed phase separation of SPAES copolymer and improved connection between the hydrophilic domains. This study concludes that the kind of hydrophobic monomers and the length of the hydrophilic segment in SPAES copolymer played a key role in the membrane performance as a proton-exchange membrane.

The authors would like to thank Prof. A. Mori at Kobe University for his help in the ¹H-NMR analyses.

References

1. Li, Y.; Wang, F.; Yang, J.; Liu, D.; Roy, A.; Case, S.; Lesko, J.; McGrath, J. E. *Polymer* 2006, 47, 4210.
2. Wang, F.; Hickner, M.; Kim, Y. S.; Zawodzinski, T.; McGrath, J. E. *J Membr Sci* 2002, 197, 231.
3. Bae, B.; Miyatake, K.; Watanabe, M. *Macromolecules* 2009, 42, 1873.
4. Kim, D. S.; Shin, K. H.; Park, H. B.; Chung, Y. S.; Nam, S. Y.; Lee, Y. M. *J Membr Sci* 2006, 278, 428.
5. Chikashige, Y.; Chikyu, Y.; Miyatake, K.; Watanabe, M. *Macromol Chem Phys* 2006, 207, 1334.
6. Park, H. B.; Lee, C. H.; Sohn, J. Y.; Lee, Y. M.; Freeman, B. D.; Kim, H. J. *J Membr Sci* 2006, 285, 432.
7. Hickner, M.; Pivovar, B. S. *Fuel Cells* 2005, 5, 213.
8. Kim, Y. S.; Einsla, B.; Sankir, M.; Harrison, W.; Pivovar, B. S. *Polymer* 2006, 47, 4026.
9. Ishikawa, J.-I.; Fujiyama, S.; Inoue, K.; Omi, T.; Tamai, S. *J Membr Sci* 2007, 298, 48.
10. Brijmohan, S. B.; Swier, S.; Weiss, R. A.; Shaw, M. T. *Ind Eng Chem Res* 2005, 44, 8039.
11. Chen, N.-P.; Hong, L. *Eur Polym J* 2001, 37, 1027.
12. Jiang, R.-C.; Kunz, H. R.; Fenton, J. M. *J Membr Sci* 2006, 272, 116.
13. Nagarale, R. K.; Gohil, G. S.; Shahi, V. K. *J Membr Sci* 2006, 280, 389.
14. Ismail, A. F.; Othman, N. H.; Mustafa, A. *J Membr Sci* 2009, 329, 18.
15. Jiang, Z.; Zheng, X.; Wu, H.; Wang, J.; Wang, Y. *J Power Sources* 2008, 180, 143.
16. Pang, J.; Zhang, H.; Li, X.; Wang, L.; Liu, B.; Jiang, Z. *J Membr Sci* 2008, 318, 271.
17. Tricoli, V. *J Electrochem Soc* 1998, 145, 3798.
18. Li, X.; Zhang, G.; Xu, D.; Zhao, C.; Na, H. *J Power Sources* 2007, 165, 701.
19. Fujimura, M.; Hashimoto, T. J.; Kawai, H. *Macromolecules* 1981, 14, 1309.
20. Storey, R. F.; Baugh, D. W. *Polymer* 2000, 41, 3205.
21. Ghassemi, H.; McGrath, J. E.; Zawodzinski, T. S., Jr. *Polymer* 2006, 47, 4132.
22. Yang, B.; Manthiram, A. *J Power Sources* 2006, 153, 29.
23. Li, Y.; Roy, A.; Badami, A. S.; Hill, M.; Yang, J.; Dunn, S.; McGrath, J. E. *J Power Sources* 2007, 172, 30.
24. Roy, A.; Yu, X.; Dunn, S.; McGrath, J. E. *J Membr Sci* 2009, 327, 118.
25. Pivovar, B. S.; Wang, Y.-X.; Cussler, E. L. *J Membr Sci* 1999, 154, 155.
26. Roy, A.; Hickner, M. A.; Yu, X.; Li, Y.; Glass, T. E.; McGrath, J. E. *J Polym Sci Part B: Polym Phys* 2006, 44, 2226.